Eur J Vasc Endovasc Surg (2010) xx, 1–8

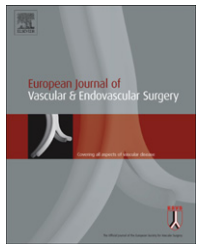

Ultrasmall Superparamagnetic Iron Oxide-enhanced Magnetic Resonance Imaging of Abdominal Aortic Aneurysms—A Feasibility Study☆

U. Sadat [a,b,*], V. Taviani [a], A.J. Patterson [a], V.E. Young [a], M.J. Graves [a], Z. Teng [a], T.Y. Tang [a,b], J.H. Gillard [a]

[a] *University Department of Radiology, University of Cambridge, Cambridge, UK*
[b] *Cambridge Vascular Unit, Cambridge University Hospitals NHS Foundation Trust, Cambridge, UK*

Submitted 27 May 2010; accepted 25 August 2010

KEYWORDS
Atheroma;
Aorta;
Aneurysm;
USPIO;
MRI;
Inflammation;
Atherosclerosis;
Macrophage

Abstract *Objectives:* Abdominal aortic aneurysms (AAAs), being predominantly atherosclerotic in nature, have underlying inflammatory activity. As it is well established that ultrasmall superparamagnetic iron oxide (USPIO) particles accumulate in the macrophages within atheromatous lesions, USPIO-enhanced magnetic resonance (MR) imaging can be potentially effective in the quantification of the associated inflammatory processes.
Methods: A total of 14 patients underwent USPIO-enhanced MR imaging using a 1.5T-MR system. Quantitative T_2* and T_2 relaxation time data were acquired before and 36 h after UPSIO infusion at identical AAA locations. The pre- and post-USPIO-infusion relaxation times (T_2^* and T_2) were quantified and the correlation between pre- and post-USPIO infusion T_2* and T_2 values was investigated.
Results: There was a significant difference between pre- and post-infusion T_2* and T_2 values (both respective p-values $= 0.005$). A significant correlation between T_2* and T_2 values post-USPIO infusion was observed ($r = 0.90$, $p < 0.001$), which indicates USPIO uptake by the aortic wall.
Conclusions: Aortic wall inflammation using USPIO-enhanced MR imaging is feasible. Use of quantitative T_2 and T_2* pulse sequences provides a quantitative method for assessing USPIO uptake by the aortic wall.

☆ This research project was funded by '*The European Society of Vascular Surgery (ESVS) Research Grant*'. The study was also supported by a Biomedical Research Centre National Institute of Health Research (BRC NIHR) grant. Dr. Umar Sadat is supported by a Medical Research Council UK & Royal College of Surgeons of England Joint Clinical Research Training Fellowship. We thank Jeff Stainsby of GE Healthcare for providing the prototype black blood electrocardiogram (ECG)-triggered multi-echo sequence for T_2 quantification and Andrew Gill for providing the quantitative relaxation measurement software used for image analysis.
* Corresponding author. U. Sadat, Box 218, Level 5, University Department of Radiology, Addenbrooke's Hospital, Hills Road, Cambridge CB2 0QQ, UK. Tel.: +44 01223 767834.
E-mail address: us229@cam.ac.uk (U. Sadat).

1078-5884/$36
doi:10.1016/j.ejvs.2010.08.022

Atherosclerosis, which was previously considered a bland lipid-storage disorder, can present as a chronic inflammatory disease, which proceeds in the context of enhanced plasma lipid levels.[1] Various cellular and molecular imaging techniques allow visualisation of these underlying inflammatory processes.[2–6] These offer new opportunities to study the evolution and biology of atherosclerotic lesions *in vivo*, as well as new clinically translatable strategies to identify high-risk atherosclerotic lesions and potentially to monitor the efficacy of anti-inflammatory medications, which are used to treat atherosclerosis.[7]

Ultrasmall superparamagnetic iron oxide (USPIO)-enhanced magnetic resonance (MR) imaging is one of these imaging techniques, which has been successfully used to identify inflammation within carotid atheroma,[8–11] and also to monitor the anti-inflammatory effect of a statin on carotid plaque stabilisation.[12] USPIO particles are believed to be taken up by the macrophages within atherosclerotic plaques, thus producing a T_2*-susceptibility effect visible as signal voids (hypointense regions) in T_2*-weighted images.[5] T_2* represents the characteristic time of transverse relaxation in the presence of magnetic field inhomogeneities. Magnetic field inhomogeneities arise from inherent imperfections in the field produced by the magnet, as well as susceptibility differences within the body and accelerate the decay of the transverse magnetisation. The degree and extent of USPIO-induced signal loss is related to the severity of the inflammation,[13] with vulnerable atherosclerotic lesions exhibiting higher USPIO-defined inflammation compared with stable ones.[14] Quantitative T_2* measurements have recently been shown to be more robust than other semi-quantitative methods (based on relative signal intensity measurements), previously used to assess USPIO uptake.[15] In addition, quantitative T_2 measurements have been suggested to be more specific than T_2* relaxation, due to their inherent insensitivity to concomitant magnetic field inhomogeneities[16] (T_2 is the characteristic time of spin–spin relaxation in the transverse plane). T_2 only depends on the exchange of energy with nearby nuclei, while T_2* is additionally affected by magnetic field inhomogeneity. Therefore, T_2* has a potential weakness in that it might not accurately reflect iron concentration in tissue because of its sensitivity to shimming and susceptibility. T_2 is potentially more specific, but has a lower sensitivity. Initial attempts to quantify iron deposition *in vivo* using T_2 were unsuccessful, mainly due to hardware limitations and problems related to motion artefacts. By contrast, T_2* measurements have increasingly been used in clinical practice because of their sensitivity to iron and good reproducibility. Recently, robust quantitative T_2 sequences[17] have become available, which substantially reduce acquisition times with respect to standard spin echo acquisitions. It should also be noted that the image quality and signal-to-noise ratio (SNR) are superior in the quantitative T_2 sequence. For this reason, we decided to measure both T_2 and T_2* as both have the potential of being used to quantify USPIO uptake.

Because abdominal aortic aneurysms (AAAs) are mostly atherosclerotic in nature and have underlying inflammatory activity,[18] USPIO-enhanced MR imaging can potentially be effective in the visualisation and quantification of the associated inflammatory processes. However, very little is known about USPIO uptake in the aortic wall.[19,20] Traditionally, aortic diameter has been used for the clinical assessment of patients with large aneurysms to identify those at higher risk of rupture. However, small aneurysms also rupture.[21,22] Therefore, USPIO-enhanced MR imaging could be used to assess inflammatory activity within aneurysms, which although small in size, may have higher inflammation and, therefore, be more prone to rupture. In this study, we assess whether USPIO uptake in AAAs can be quantified using both T_2*- and T_2- relaxation measurements.

Methods

Fourteen patients with an infra-renal AAA were recruited from the Cambridge Vascular Unit. All patients were undergoing serial ultrasound imaging of their AAAs as part of the UK-based AAA screening programme. The research project had ethics approval from the Regional Research and Ethics Committee and the Medicines and Healthcare products Regulatory Agency (MHRA). All patients gave written informed consent.

The inclusion criteria for the study were:

(1) patient age 18–90 years;
(2) known infra-renal AAAs (>4.0 cm to <5.5 cm), under regular surveillance;
(3) not being considered for surgery or endovascular treatment; and
(4) subjects must give signed written informed consent before beginning study-related procedures.

The exclusion criteria included:

(1) history of atopy, asthma, allergic reaction to contrast materials and allergy to iron and dextran;
(2) documented history of renal impairment (estimated glomerular filtration rate <60 ml min^{-1} 1.73 m^{-2});
(3) documented history of haemochromatosis; and
(4) contraindication to MR imaging such as metallic joint replacements and cardiac pacemaker.

Pre-USPIO infusion MR imaging

MR images before and after USPIO infusion were acquired using a 1.5T-MR system (Signa HDx, GE Healthcare, Waukesha, WI, USA) and an eight-channel phased-array cardiac coil. Axial and coronal fast imaging employing steady-state acquisition (FIESTA) images covering the infra-renal AAA (slice thickness: 6 mm) were acquired to identify the aneurysm shoulder (defined as the site where the normal aorta joins the aneurysmal section), which is believed to be a location of maximum structural weakness.[23–28] A two-dimensional (2D), fat-suppressed, single breath-hold, double inversion recovery (DIR)-prepared fast spin echo (FSE) pulse sequence effective echo time (TEeff) = 6.7 ms; repetition time (TR) = 1 × RR; echo train length (ETL) = 12 was used to produce 3–5 axial T_1-weighted images covering the aneurysm shoulder (voxel size = 0.625 × 0.625 × 5 mm).

Please cite this article in press as: Sadat U, et al., Ultrasmall Superparamagnetic Iron Oxide-enhanced Magnetic Resonance Imaging of Abdominal Aortic Aneurysms–A Feasibility Study, Eur J Vasc Endovasc Surg (2010), doi:10.1016/j.ejvs.2010.08.022

Quantitative T_2* data were acquired covering the aneurysm shoulder at the same slice location as T_1-weighted images, with no inter-slice gap, using a 2D, ECG-triggered, single breath-hold, multi-echo, segmented *k*-space fast gradient echo pulse sequence (MFGRE, GE Healthcare, Waukesha, WI, USA) which was modified in-house to include DIR preparation. Eight echoes, with TEs ranging from 3.2 ms to 41 ms at 5.4 ms increments were acquired. The TEs for the T_2* acquisition were selected on the basis of prior T_2* measurements performed in carotid plaques pre- and post-USPIO infusion.[15] Other imaging parameters were: TR = 1 × RR; flip angle = 20°; slice thickness = 5 mm; matrix size = 256^2; views-per-segment = 8. Quantitative T_2 data were acquired at the same slice location as T_1-weighted images, using a prototype 2D DIR-prepared, single breath-hold multi-echo FSE pulse sequence (MEFSE, GE Healthcare, Waukesha, WI, USA). Four echoes with TEs at 4.5, 22.5, 40.8 and 58.8 ms were acquired. Other imaging parameters were TR = 1 × RR; ETL = 16; slice thickness = 5 mm; matrix size = 256 × 192; parallel imaging acceleration factor = 2. The reason for using 5-mm slice thickness was that because the aorta was located approximately midway between the two coil elements, images were intrinsically characterised by low SNR. A thinner slice thickness would have reduced partial voluming effects in the slice-select direction at the expense of a reduction in SNR. A 5-mm slice thickness was considered as a good compromise to produce relatively high-SNR images while ensuring limited partial voluming effects in the slice-select direction. The imaging field of view for the T_2* and T_2 acquisitions was chosen on a per patient basis and ranged between 24 and 42 cm.

USPIO infusion

Following the baseline MR imaging of AAA, patients were given an infusion of Sinerem™ (Guerbet, Roissy, France), a USPIO contrast agent. The compound was supplied as a dry powder and initially made up to a volume of 15 ml with normal saline. An appropriate weight-calculated dose was then measured. The dose used was 2.6 mg Fe kg^{-1}. The contrast agent was further diluted in 100 ml of normal saline and given as a slow infusion through a large-bore intravenous cannula over a period of 30 min. Safety data for this contrast agent have previously been published.[12]

Post-USPIO infusion MR imaging

AAA MR imaging was repeated 36 h following USPIO infusion. The optimum time window for MR imaging post-USPIO infusion has been previously determined to be between 36 and 48 h.[29] Post-infusion T_1-weighted, T_2* and T_2 images were acquired at the same AAA locations as for the baseline MR imaging. Slice locations between pre- and post-USPIO infusion were matched taking the distance from the renal arteries or the aortic bifurcation as a reference. A Modified Look Locker Inversion recovery (MOLLI) sequence was used to obtain quantitative T_1 measurements of the blood pool post-infusion to optimise the inversion time (TI) in the DIR-prepared pulse sequences,[30] due to the reduction in the T_1 of blood following USPIO infusion. The other imaging parameters were chosen to match the baseline MR imaging.

MR image analysis

Images were analysed with software developed in-house using Matlab version 7.5.0 (The Mathworks, Inc., Natick, MA, USA). Regions of interest (ROIs) delineating the wall/lumen interface and the external aneurysmal wall were manually drawn on T_2 images pre- and post-USPIO infusion. The same ROIs were copied to the corresponding T_2* images. Both T_2* and T_2 images were analysed on a segmental basis whereby each ROI was divided into six radial segments (Fig. 1). For each segment, the mean signal intensity for each echo time was measured and plotted as a function of the echo time to obtain a signal decay curve. The Miller correction, to account for non-zero background signal intensity,[31] and a non-linear curve-fitting algorithm[32] were used to fit an exponential decay model to each data set to derive the proton density (M_0) and corresponding T_2* or T_2 relaxation times. A similar analysis was performed on a per-pixel basis to produce T_2* and T_2 maps and histograms over each ROI.

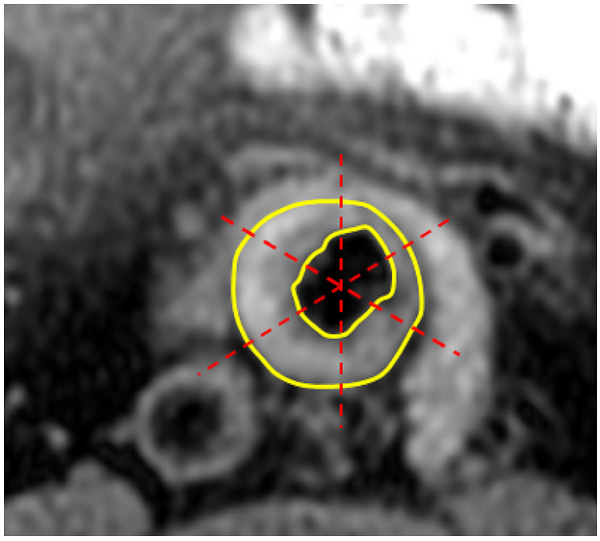

Figure 1 An axial MR slice with 6 regions of interest (ROIs) drawn on it. There were 3—5 ROIs per patient, depending on the number of slices (N) used to cover the aneurysm shoulder. In the segmental analysis, each ROI was divided into 6 segments so that 6 × N segments were analysed for each patient. Maps and histograms were produced for each ROI so that the number of maps/histograms per patient was equal to the number of slices used to cover the aneurysm shoulder. In the statistical analysis, we always considered a single metric per patient so that no correction was necessary. In the segmental analysis, we considered the average T_2 and T_2* values over all the segments and slices for each patient. In the histogram analysis, the average median value over the three slices was considered.

Please cite this article in press as: Sadat U, et al., Ultrasmall Superparamagnetic Iron Oxide-enhanced Magnetic Resonance Imaging of Abdominal Aortic Aneurysms—A Feasibility Study, Eur J Vasc Endovasc Surg (2010), doi:10.1016/j.ejvs.2010.08.022

Table 1 Patient demographics ($n = 14$) reporting mean ± standard deviation.

Patient demographics	mean SD
Age [yrs]	75 ± 7
Hypertension [%]	6 ± 46
Diabetes [%]	None
Renal impairment [%]	None
Peripheral vascular Disease [%]	3 ± 23
Ischaemic heart disease [%]	6 ± 46
Current Smokers [%]	6 ± 46
Ex-smokers [%]	7 ± 54
Heart Rate [beats/min]	68 ± 10
Systolic blood pressure mmHg [mmHg]	138 ± 26
Diastolic blood pressure mmHg [mmHg]	80 ± 10
AAA growth rate [mm/yr]	3.93 ± 2.53
Patients on aspirin (dose: 75 mg per day)	100%
Patients on statins [mean dose = 40 mg (Simvastatin equivalent)]	100%

Statistical analysis

Normally distributed summary data are reported as mean ± standard deviation. Differences between T_2* and T_2 pre- and post-infusion were assessed by a paired two-sided *t*-test or a Welch test when variances were different according to the *F*-test. Spearman's correlation coefficients were used to measure the strength of correlation between T_2* and T_2 pre- and post-USPIO infusion. Simple linear regression was used to determine the relationship between ΔT_2* and ΔT_2 and the aneurysm growth rate. A *p*-value of less than 0.05 was considered statistically significant. The analysis was performed using the statistical programming language R version 2.5.1 (The R Foundation for Statistical Computing, Vienna, Austria).

Results

Of the 14 patients recruited, 13 patients successfully completed the study and were included in data analysis. One T_2* data set pre-USPIO and three T_2* data sets post-infusion were discarded due to poor image quality. T_2 data sets (pre- and post-infusion) of all 13 patients had good image quality and were used for analysis. The average age of the patients was 75 ± 7 years. The majority of the patients were male ($n = 12$, 92%). The patient demographics are presented in Table 1. The average imaging time was 40 ± 8 min for the first MR session and 50 ± 15 min for the second MR imaging session. The second imaging session included the MOLLI sequence to obtain quantitative T1 measurements of the blood pool post-infusion and acquisition of additional scout images to ensure co-localisation with respect to the first imaging session. This explains the slightly longer imaging time in the second visit.

Segmental T_2* and T_2 values pre- and post-USPIO infusion were significantly different (both respective *p*-values = 0.005; pre-infusion T_2* = 37.8 ± 13.5 ms; T_2 = 56.4 ± 14.7 ms; post-infusion T_2* = 20.4 ± 8.8 ms; T_2 = 35.8 ± 13.8 ms). The median T_2* and T_2 as determined from the per-slice histogram analysis also changed significantly following USPIO infusion (both respective *p*-values = 0.005). Distributions of the average T_2 and T_2* values over the six segments pre- and post-infusion are shown in Fig. 2(a) and (b), respectively.

No correlation between segmental T_2* and T_2 values either pre- or post-infusion was found; however, the histogram analysis revealed a significant correlation between T_2* and T_2 values post-infusion, but no correlation between the corresponding values pre-infusion when comparing the histograms median values (pre-infusion: $r = 0.27$; *p*-value = 0.44; post-infusion: $r = 0.90$; *p*-value <0.001; Fig. 3). Two of the 14 patients, who participated in the study, had intraluminal thrombus (ILT). Figs. 4 and 5 show the T_1-weighted images and the first echoes from the T_2 and T_2* acquisitions pre- and post-infusion as well as the corresponding T_2 maps and FIESTA images. The case reported in Fig. 4 shows a significant reduction in T_2 values within the ILT, suggesting a higher degree of USPIO uptake and, hence, inflammation in this region than in the adjacent aortic wall. By contrast, the case shown in Fig. 5, while characterised by a small T_2 variation between pre- and post-infusion, showed a marked T_1 effect (hyperintensity) on T_1-weighted images, which probably reflects a relatively lower degree of USPIO uptake.[33]

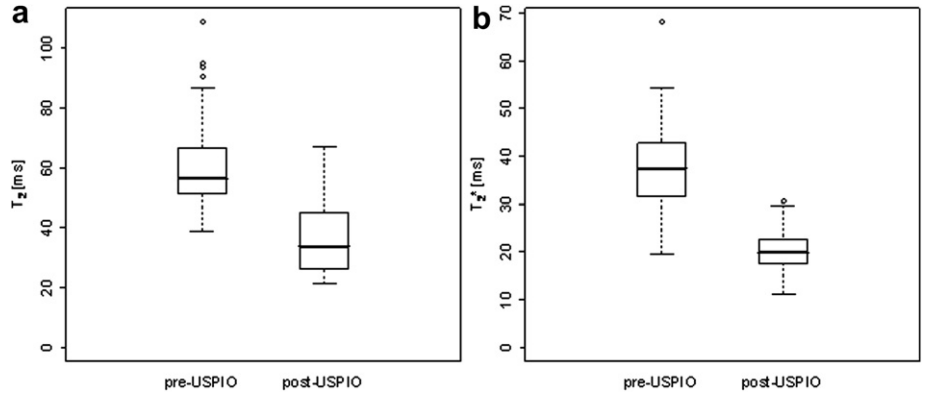

Figure 2 Box and whisker plots of the average T_2 (a) and T_2* (b) values over the 6 segments pre and post-infusion. T_2 values pre and post-infusion were significantly different ($p = 0.005$). The same was true for T_2* values ($p = 0.005$).

Please cite this article in press as: Sadat U, et al., Ultrasmall Superparamagnetic Iron Oxide-enhanced Magnetic Resonance Imaging of Abdominal Aortic Aneurysms—A Feasibility Study, Eur J Vasc Endovasc Surg (2010), doi:10.1016/j.ejvs.2010.08.022

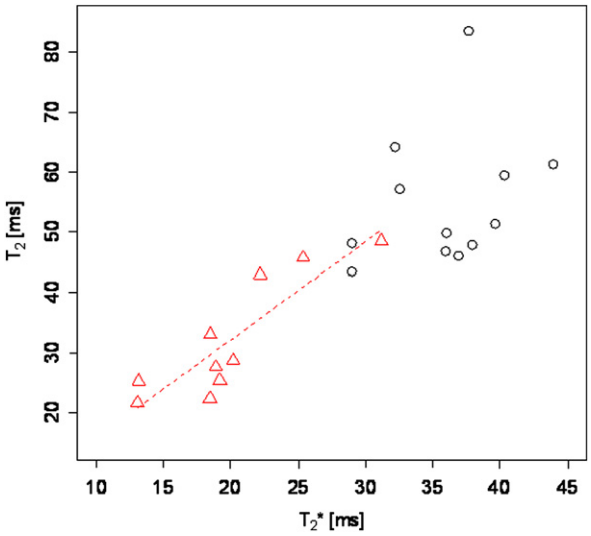

Figure 3 Correlation between the cross-sectional median T_2* and T_2 values as derived from the histogram analysis. There was no correlation between T_2* and T_2 values pre-USPIO infusion (black circles). A significant correlation was found between T_2* and T_2 values post-USPIO infusion (red triangles, Spearman's correlation coefficient $= 0.90$ [p-value < 0.001]). Similar results were obtained when considering the histogram mean and mode values.

Discussion

As degradation of the extracellular matrix within the aortic wall is responsible for the 'terminal event' of AAA rupture,[34] visualisation/quantification of the associated aortic wall inflammatory activity could potentially be used for the rupture-risk assessment of AAAs. USPIO-enhanced MR imaging has been used extensively for the assessment of the underlying inflammatory activity in atherosclerotic plaques,[5] and also seems to have the potential for investigating the aetiopathology of AAA.[19,35–37] In this study, for the first time, USPIO uptake by the AAA wall was quantified using both T_2* and T_2 relaxation measurements. Previously, Truijers *et al*. have reported the use of USPIO-enhanced MR imaging for the assessment of inflammation in the human aortic wall.[20] However, they acquired MRI data post-USPIO, and performed a semi-quantitative analysis technique. which involved counting the number of quadrants characterised by USPIO-induced signal loss as a marker of inflammation. Whilst similar semi-quantitative approaches have been widely employed, they have been criticised in a recent editorial, which highlights problems associated with interpreting a semi-quantitative metric as a meaningful pseudo-marker for inflammation.[38] An alternative approach is to quantify the change in T_2* relaxation time of the aortic wall directly, by multi-echo gradient echo imaging. USPIO uptake by activated macrophages within

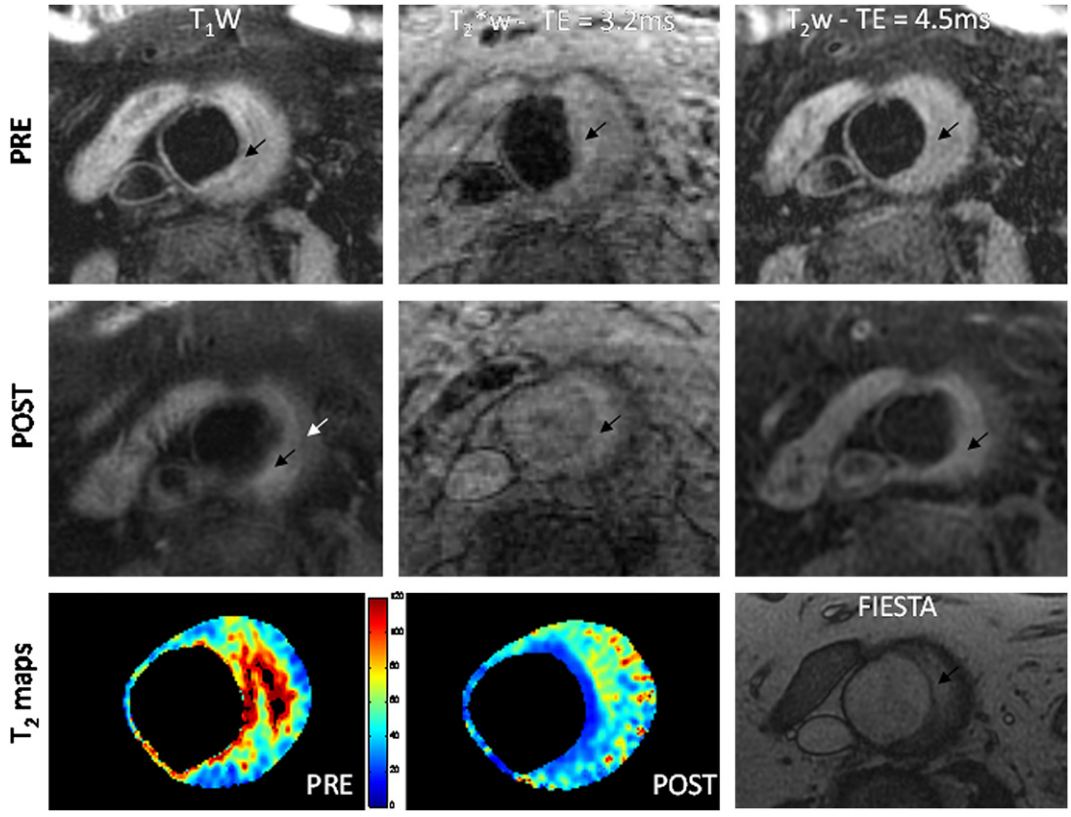

Figure 4 T_1-weighted images and first echoes from the T_2* and T_2 acquisitions pre and post-infusion as well as the corresponding T_2 maps and FIESTA images. T_2 values following USPIO infusion were considerably lower than T_2 values pre-USPIO infusion. The region characterised by the greatest T_2 change was approximately coincident with the thrombus region (black arrow), suggesting a high degree of USPIO uptake and hence inflammation in this region, compared to the adjacent aortic wall (white arrow).

Please cite this article in press as: Sadat U, et al., Ultrasmall Superparamagnetic Iron Oxide-enhanced Magnetic Resonance Imaging of Abdominal Aortic Aneurysms—A Feasibility Study, Eur J Vasc Endovasc Surg (2010), doi:10.1016/j.ejvs.2010.08.022

the inflamed tissue produces a localised susceptibility artefact, which can be quantified in terms of T_2* shortening. Although T_2* relaxivity is more sensitive to variations in USPIO concentration, this technique has previously received criticism due to its intrinsic sensitivity to magnetic field inhomogeneities. Which. in principle. can lead to inaccurate T_2* measurements.[39] In this study, we measured both T_2 and T_2* relaxivities and found them to be significantly correlated post-USPIO infusion. This confirmed previous work by He *et al.*[16] who reported a strong linear correlation between myocardial T_2 and T_2* values in iron-overloaded patients, and no correlation in healthy volunteers. Likewise, the post-USPIO-infusion correlation between T_2 and T_2* values observed in our study indicates USPIO uptake within the aortic wall.

We did not observe any correlation between the segmental T2 and T2* values pre- and post-infusion. There was no correlation pre-infusion, as there is not a common dominating factor in determining T_2 and T_2* values. The reason why we did not find any correlation between segmental T_2 and T_2* values post-infusion is probably a consequence of assuming normally distributed values within each segment. The histogram analysis showed that T_2* values were not normally distributed due to the presence of outliers produced by artefacts in the original MFGRE images. When considering the histograms median values, more representative of the underlying actual distribution, a significant correlation was found between T_2 and T_2* values post-USPIO infusion. Histograms were produced to allow further investigation of the distribution of T_2 and T_2* values on a per-slice basis.

We also observed that the over all image quality of the MEFSE pulse sequence was superior to that of the MFGRE sequence with fewer outliers in the resulting T_2 and T_2* values. This is probably because the MEFSE pulse sequence is inherently insensitive to field inhomogeneities. Although T_2 is less sensitive to variations in USPIO concentrations, the T_2 reduction between pre- and post-imaging sessions was still significant. These features probably make MEFSE the preferred pulse sequence for quantitative USPIO imaging.

As mentioned in the results, a T_1 effect was observed following USPIO imaging, we did not attempt any quantitative T_1 measurement in this study. However, recent experiments performed by our group in USPIO-containing gels showed that, at low concentrations of USPIO, there is an observable increase in signal intensity attributed to the USPIO nanoparticles shortening the T_1 relaxation time of protons in the vicinity of the USPIO nanoparticles. As the concentration of USPIO increases further, T_2* dephasing starts to dominate, and there is an observable decrease in signal intensity.[15] This effect was responsible for the signal

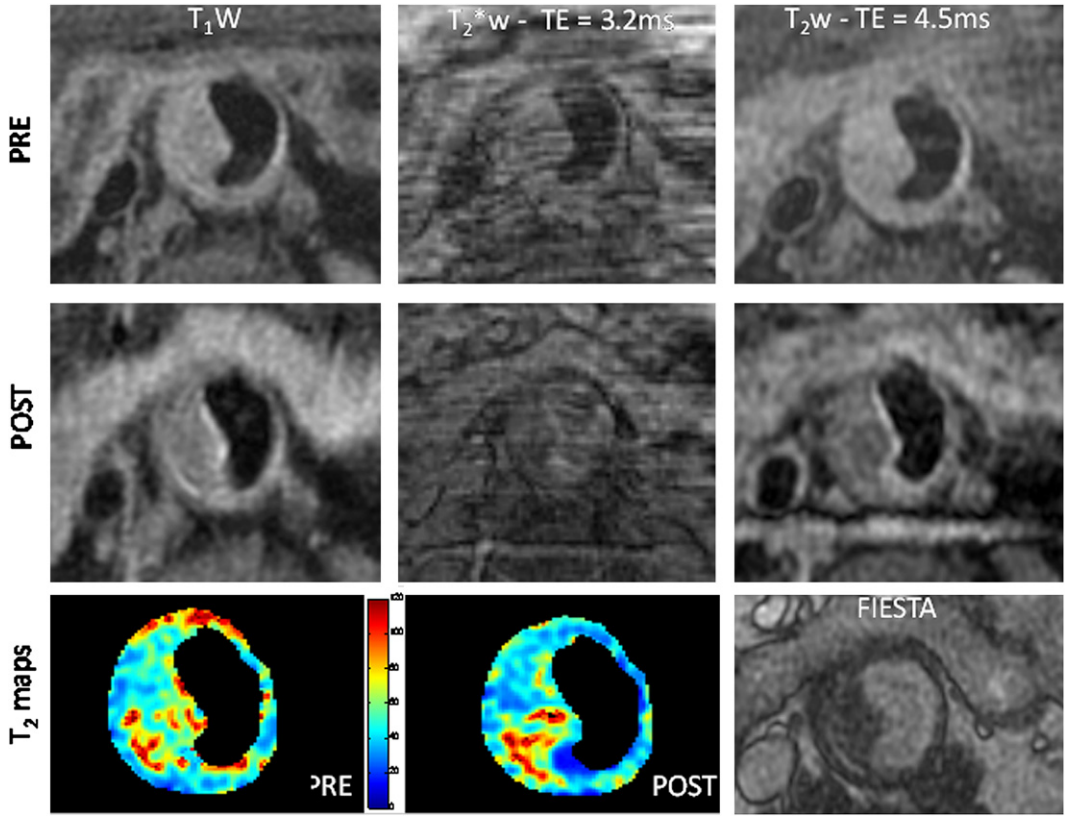

Figure 5 T_1-weighted images and first echoes from the T_2* and T_2 acquisitions pre and post-infusion as well as the corresponding T_2 maps and FIESTA images. Unlike the case reported in Figure 3, T_2 maps pre and post-infusion were relatively similar, reflecting low USPIO-defined inflammation in the thrombus (black arrow) in this patient. The limited USPIO uptake observed in this case was confirmed by the presence of a marked T_1 effect (hyperintensity lining the thrombus shown by white arrow) visible on T_1-weighted images.

Please cite this article in press as: Sadat U, et al., Ultrasmall Superparamagnetic Iron Oxide-enhanced Magnetic Resonance Imaging of Abdominal Aortic Aneurysms—A Feasibility Study, Eur J Vasc Endovasc Surg (2010), doi:10.1016/j.ejvs.2010.08.022

enhancement previously observed in asymptomatic carotid plaques after USPIO infusion.[33] The case shown in Fig. 5 was characterised by a small T_2/T_2* variation between pre- and post-infusion measurement, suggesting a low degree of USPIO uptake. This was further confirmed by the localised signal enhancement in proximity to the fibrous cap visible on both T_2- and T_2*-weighted images, which, due to the TR of 1 $\times$ RR, also had some degree of T1 weighting, thus explaining the signal hyperintensity.

In general, we also observed excellent patient compliance, with none of the patients having any USPIO-infusion-related adverse effects. Although the breath-holds used for the MR pulse sequences varied from 8 to 30 s, none of the research subjects withdrew from the study due to poor compliance. Only one patient withdrew from the study after the pre-USPIO imaging, and this was due to general frailty.

We believe this study to be the first to report quantitative T_2* and T_2 relaxation times pre- and post-USPIO in AAA, and as a feasibility study, it provides useful information, which can be used for planning large-scale studies in future, aimed at imaging inflammation within the aortic wall with novel agents. However, it has some limitations. One limitation is the lack of histology; but obtaining reliable MR image co-registration or correlation with histological sections would require excision of the entire aneurysm (aneurysmectomy), which is not routinely performed in clinical practice. Using punch or wedge biopsies to get histological information may not provide useful data for MR image correlation purposes because the general heterogeneity of USPIO uptake as shown in the T_2 maps demonstrates how difficult it would be to sample an appropriate region. Second, as USPIO can be taken up by the lymph nodes (such as periaortic lymph nodes), due to close proximity of the periaortic lymph nodes to the aortic wall, blooming (resulting from T_2*) may impair the discrimination between signal loss in atherosclerotic plaques and signal loss from the lymph nodes. However, we did not observe this in our patients. Lastly, the USPIO agent used in this study is no longer commercially available. However, the technical development done in this study can be used in future studies using other USPIO agents, which are being developed.

Conclusions

Imaging aortic wall inflammation using UPSIO-enhanced MRI is clinically feasible. Use of quantitative T_2 and T_2* pulse sequences provides a quantitative method for assessing USPIO uptake by the aortic wall, which is suggestive of underlying inflammation within abdominal aortic aneurysms. Future studies should focus on using these imaging protocols to assess the relationship between aneurysm expansion and USPIO-defined inflammation in larger patient cohorts. This may help us assess the efficacy of various anti-inflammatory medications in dose—response studies in future. The effectiveness and use of USPIO-enhanced MR imaging in routine clinical practice remains to be established compared with the standard clinical follow-up and duplex ultrasound screening.

Conflict of Interest

None.

References

1 Libby P. Inflammation in atherosclerosis. *Nature* 2002;**420**:868—74.
2 Jaffer FA, Weissleder R. Molecular imaging in the clinical arena. *JAMA* 2005;**293**:855—62.
3 Choudhury RP, Fisher EA. Molecular imaging in atherosclerosis, thrombosis, and vascular inflammation. *Arterioscler Thromb Vasc Biol* 2009;**29**:983—91.
4 Rudd JH, Hyafil F, Fayad ZA. Inflammation imaging in atherosclerosis. *Arterioscler Thromb Vasc Biol* 2009;**29**:1009—16.
5 Tang TY, Muller KH, Graves MJ, Li ZY, Walsh SR, Young V, et al. Iron oxide particles for atheroma imaging. *Arterioscler Thromb Vasc Biol*; 2009.
6 Sadat U, Li ZY, Graves MJ, Tang TY, Gillard JH. Noninvasive imaging of atheromatous carotid plaques. *Nat Clin Pract Cardiovasc Med* 2009;**6**:200—9.
7 Jaffer FA, Libby P, Weissleder R. Optical and multimodality molecular imaging: insights into atherosclerosis. *Arterioscler Thromb Vasc Biol* 2009;**29**:1017—24.
8 Tang TY, Howarth SP, Miller SR, Graves MJ, UK-I JM, Li ZY, et al. Correlation of carotid atheromatous plaque inflammation using uspio-enhanced mr imaging with degree of luminal stenosis. *Stroke* 2008;**39**:2144—7.
9 Tang TY, Moustafa RR, Howarth SP, Walsh SR, Boyle JR, Li ZY, et al. Combined pet-fdg and uspio-enhanced mr imaging in patients with symptomatic moderate carotid artery stenosis. *Eur J Vasc Endovasc Surg* 2008;**36**:53—5.
10 Trivedi RA, Mallawarachi C, U. King-Im JM, Graves MJ, Horsley J, Goddard MJ, et al. Identifying inflamed carotid plaques using in vivo uspio-enhanced mr imaging to label plaque macrophages. *Arterioscler Thromb Vasc Biol* 2006;**26**:1601—6.
11 Trivedi RA, UK-I JM, Graves MJ, Kirkpatrick PJ, Gillard JH. Noninvasive imaging of carotid plaque inflammation. *Neurology* 2004;**63**:187—8.
12 Tang TY, Howarth SP, Miller SR, Graves MJ, Patterson AJ, UK-I JM, et al. The atheroma (atorvastatin therapy: effects on reduction of macrophage activity) study. Evaluation using ultrasmall superparamagnetic iron oxide-enhanced magnetic resonance imaging in carotid disease. *J Am Coll Cardiol* 2009;**53**:2039—50.
13 Trivedi RA, Mallawarachi C, UK-I JM, Graves MJ, Horsley J, Goddard MJ, et al. Identifying inflamed carotid plaques using in vivo uspio-enhanced mr imaging to label plaque macrophages. *Arterioscler Thromb Vasc Biol* 2006;**26**:1601—6.
14 Howarth SP, Tang TY, Trivedi R, Weerakkody R, UK-I J, Gaunt ME, et al. Utility of uspio-enhanced mr imaging to identify inflammation and the fibrous cap: a comparison of symptomatic and asymptomatic individuals. *Eur J Radiol*; 2008.
15 Patterson AJ, Tang TY, Graves MJ, Müller KH, Gillard JH. In vivo carotid plaque magnetic resonance imaging using quantitative t2* measurements with uspio particles: a dose-response study to statin therapy NMR in Biomedicine, in press.
16 He T, Smith GC, Gatehouse PD, Mohiaddin RH, Firmin DN, Pennell DJ. On using t2 to assess extrinsic magnetic field inhomogeneity effects on t2* measurements in myocardial siderosis in thalassemia. *Magn Reson Med* 2009;**61**:501—6.
17 He T, Gatehouse PD, Anderson LJ, Tanner M, Keegan J, Pennell DJ, et al. Development of a novel optimized breathhold technique for myocardial t2 measurement in thalassemia. *J Magn Reson Imaging* 2006;**24**:580—5.

Please cite this article in press as: Sadat U, et al., Ultrasmall Superparamagnetic Iron Oxide-enhanced Magnetic Resonance Imaging of Abdominal Aortic Aneurysms—A Feasibility Study, Eur J Vasc Endovasc Surg (2010), doi:10.1016/j.ejvs.2010.08.022

18 Golledge J, Muller J, Daugherty A, Norman P. Abdominal aortic aneurysm: pathogenesis and implications for management. *Arterioscler Thromb Vasc Biol* 2006;**26**:2605–13.
19 Howarth SP, Tang TY, Graves MJ, UK-I JM, Li ZY, Walsh SR, et al. Non-invasive mr imaging of inflammation in a patient with both asymptomatic carotid atheroma and an abdominal aortic aneurysm: a case report. *Ann Surg Innov Res* 2007;**1**:4.
20 Truijers M, Futterer JJ, Takahashi S, Heesakkers RA, Blankensteijn JD, Barentsz JO. In vivo imaging of the aneurysm wall with mri and a macrophage-specific contrast agent. *AJR Am J Roentgenol* 2009;**193**:W437–41.
21 Darling RC, Messina CR, Brewster DC, Ottinger LW. Autopsy study of unoperated abdominal aortic aneurysms. The case for early resection. *Circulation* 1977;**56**:II161–4.
22 Nicholls SC, Gardner JB, Meissner MH, Johansen HK. Rupture in small abdominal aortic aneurysms. *J Vasc Surg* 1998;**28**:884–8.
23 Matsumura JS, Chaikof EL. Continued expansion of aortic necks after endovascular repair of abdominal aortic aneurysms. Evt investigators. Endovascular technologies, inc. *J Vasc Surg* 1998; **28**:422–30 [discussion 430–421].
24 Crawford ES, Saleh SA, Babb 3rd JW, Glaeser DH, Vaccaro PS, Silvers A. Infrarenal abdominal aortic aneurysm: factors influencing survival after operation performed over a 25-year period. *Ann Surg* 1981;**193**:699–709.
25 Stringfellow MM, Lawrence PF, Stringfellow RG. The influence of aorta-aneurysm geometry upon stress in the aneurysm wall. *J Surg Res* 1987;**42**:425–33.
26 Edwards JM, Teefey SA, Zierler RE, Kohler TR. Intraabdominal paraanastomotic aneurysms after aortic bypass grafting. *J Vasc Surg* 1992;**15**:344–50 [discussion 351–343].
27 Lipski DA, Ernst CB. Natural history of the residual infrarenal aorta after infrarenal abdominal aortic aneurysm repair. *J Vasc Surg* 1998;**27**:805–11 [discussion 811–802].
28 Malina M, Ivancev K, Chuter TA, Lindh M, Lanne T, Lindblad B, et al. Changing aneurysmal morphology after endovascular grafting: relation to leakage or persistent perfusion. *J Endovasc Surg* 1997;**4**:23–30.
29 Tang TY, Patterson AJ, Miller SR, Graves MJ, Howarth SP, UK-I JM, et al. Temporal dependence of in vivo uspio-enhanced mri signal changes in human carotid atheromatous plaques. *Neuroradiology* 2009;**51**:457–65.
30 Messroghli DR, Greiser A, Frohlich M, Dietz R, Schulz-Menger J. Optimization and validation of a fully-integrated pulse sequence for modified look-locker inversion-recovery (molli) t1 mapping of the heart. *J Magn Reson Imaging* 2007;**26**:1081–6.
31 Miller AJ, Joseph PM. The use of power images to perform quantitative analysis on low snr mr images. *Magn Reson Imaging* 1993;**11**:1051–6.
32 Marquardt DW. An algorithm for least-squares estimation of nonlinear parameters. *SIAM J Appl Math* 1963;**11**:431–41.
33 Howarth SP, Tang TY, Trivedi R, Weerakkody R, UK-I J, Gaunt ME, et al. Utility of uspio-enhanced mr imaging to identify inflammation and the fibrous cap: a comparison of symptomatic and asymptomatic individuals. *Eur J Radiol* 2009;**70**: 555–60.
34 Allaire E, Schneider F, Saucy F, Dai J, Cochennec F, Michineau S, et al. New insight in aetiopathogenesis of aortic diseases. *Eur J Vasc Endovasc Surg* 2009;**37**:531–7.
35 Hyafil F, Laissy JP, Mazighi M, Tchetche D, Louedec L, Adle-Biassette H, et al. Ferumoxtran-10-enhanced mri of the hypercholesterolemic rabbit aorta: relationship between signal loss and macrophage infiltration. *Arterioscler Thromb Vasc Biol* 2006;**26**:176–81.
36 Ruehm SG, Corot C, Vogt P, Kolb S, Debatin JF. Magnetic resonance imaging of atherosclerotic plaque with ultrasmall superparamagnetic particles of iron oxide in hyperlipidemic rabbits. *Circulation* 2001;**103**:415–22.
37 Schmitz SA, Coupland SE, Gust R, Winterhalter S, Wagner S, Kresse M, et al. Superparamagnetic iron oxide-enhanced mri of atherosclerotic plaques in watanabe hereditable hyperlipidemic rabbits. *Invest Radiol* 2000;**35**:460–71.
38 Fayad ZA, Razzouk L, Briley-Saebo KC, Mani V. Iron oxide magnetic resonance imaging for atherosclerosis therapeutic evaluation: still "Rusty?". *J Am Coll Cardiol* 2009;**53**:2051–2.
39 Brittenham GM, Nathan DG, Olivieri NF, Pippard MJ, Weatherall DJ. Deferiprone versus desferrioxamine in thalassaemia, and t2* validation and utility. *Lancet* 2003;**361**:183 [author reply 183–184].

Please cite this article in press as: Sadat U, et al., Ultrasmall Superparamagnetic Iron Oxide-enhanced Magnetic Resonance Imaging of Abdominal Aortic Aneurysms–A Feasibility Study, Eur J Vasc Endovasc Surg (2010), doi:10.1016/j.ejvs.2010.08.022